Supplementary Material for

Two-dimensional biomass-derived carbon nanosheets and MnO/carbon electrodes for high-performance Li-ion capacitors

Yuemei Zhao, Yongpeng Cui, Jing Shi, Wei Liu, Zhicheng Shi,* Shougang Chen, Xin Wang, and Huanlei Wang*

Institute of Materials Science and Engineering, Ocean University of China, Qingdao 266100, China.

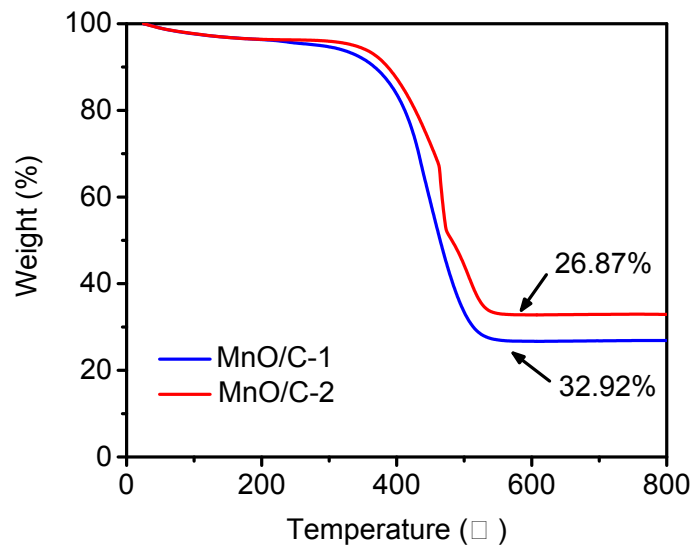*Email: huanleiwang@gmail.com; zcshi@ouc.edu.cn

Fig. S1 Thermogravimetric curves of MnO/C samples in air atmosphere. During heating in air, the MnO oxidizes to Mn_2O_3 and the carbon burns. The differential weight gain is used to calculate the MnO content in MnO/C-1 and MnO/C-2 composites.
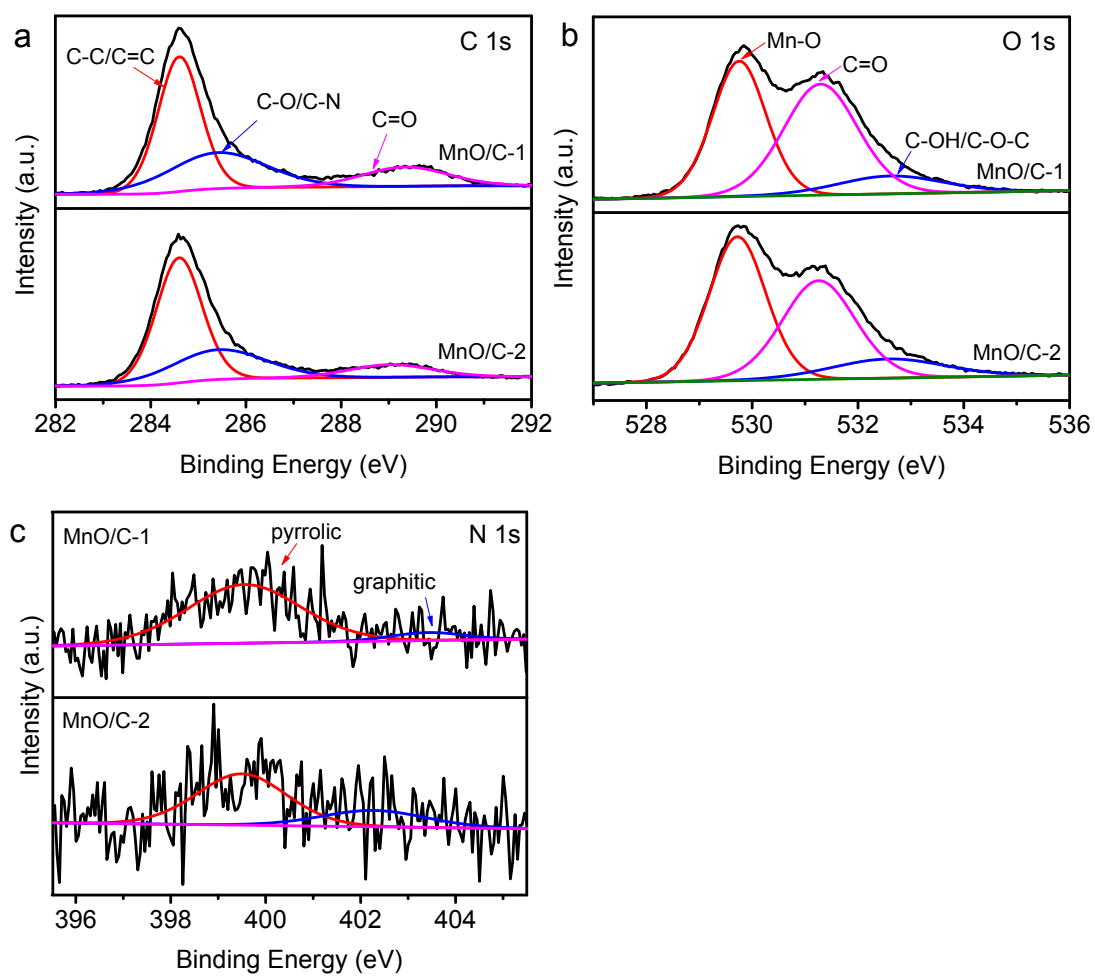
Fig. S2 High-resolution XPS (a) C 1s, (b) O 1s, (c) N 1s spectra in MnO/C-1 and MnO/C-2 samples.

Table S1. Physical parameters for CNS, MnO/C-1 and MnO/C-2.

Sample	S_{BET} (m^2 g^{-1})[a]	V_t (cm^3 g^{-1})[b]	pore vol (%)[c]		
			$V_{<1\ nm}$	$V_{1-2\ nm}$	$V_{>2\ nm}$
CNS	2056	1.83	12.1	18.8	69.1
MnO/C-1	198	0.21	10.0	17.2	72.8
MnO/C-2	157	0.15	14.5	22	63.5

[a] The specidic surface area was calculated by Brunauer-Emmett-Teller (BET) method.

[b] The total pore volume was determined at a relative pressure of 0.99.

[c] The volumes of pores smaller than 1nm ($V_{<1\ nm}$), pores between 1 and 2 nm ($V_{1-2\ nm}$), and pores large than 2 nm ($V_{>2\ nm}$) were generated by density functional theory (DFT) analysis.
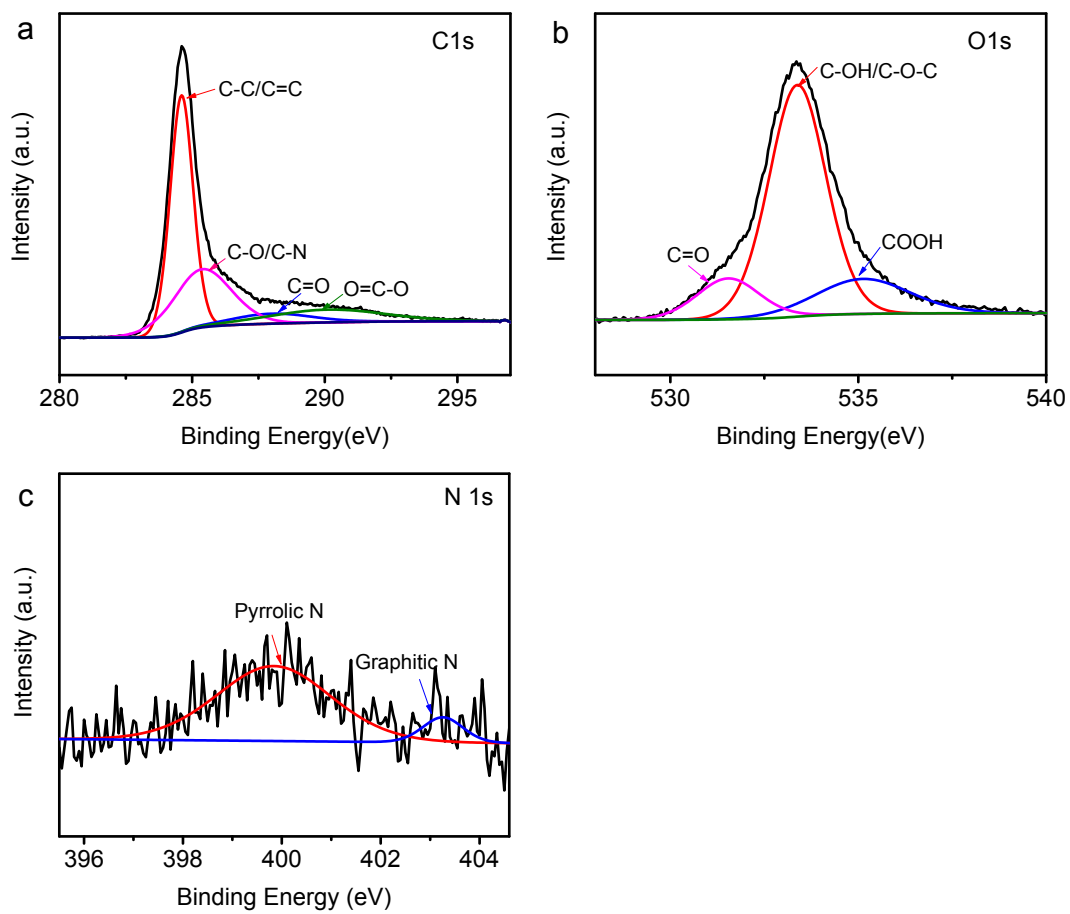
Fig. S3 High resolution XPS (a) C 1s, (b) O 1s, (c) N 1s spectra for CNS sample.
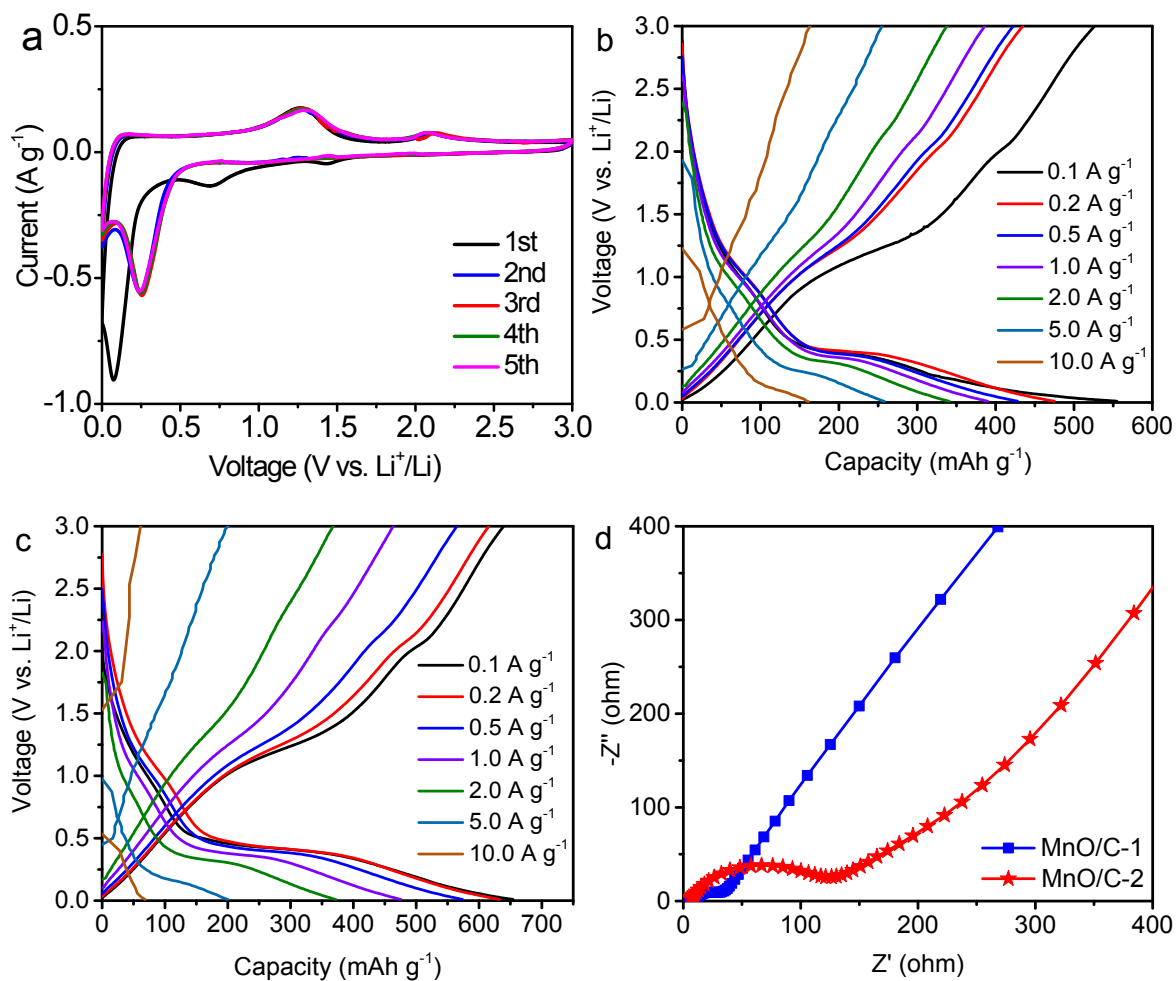
Fig. S4 (a) CV curves of MnO/C-2 at a scan rate of 0.1 mV s^{-1}. (b) Charge and discharge curves of MnO/C-1 in every fifth cycle at various current densities. (c) Charge and discharge curves of MnO/C-2 in every fifth cycle at various current densities. (d) Electrochemical impedance spectra of MnO/C samples after 500 cycles at 1 A g^{-1}.
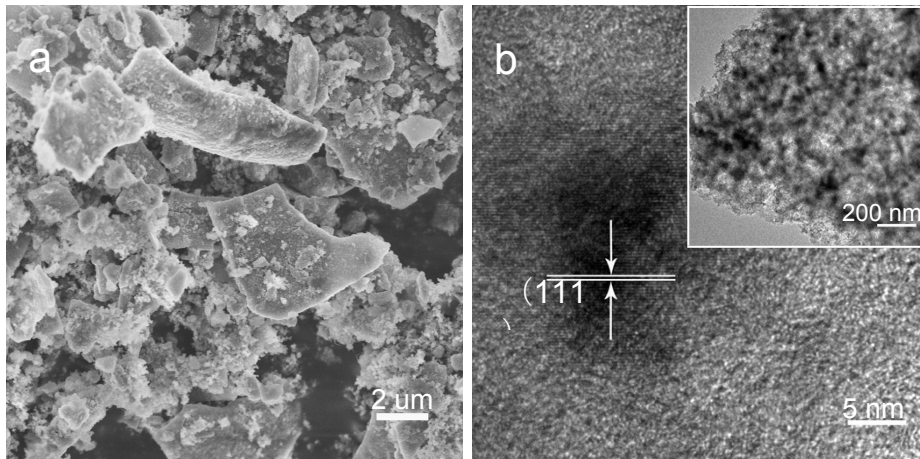
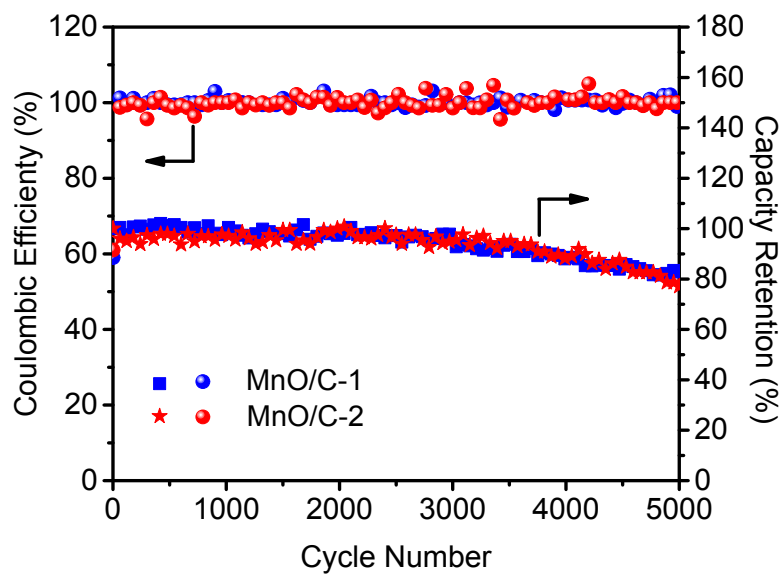**Fig. S5** (a) SEM image of MnO/C-1 electrode after 500 cycles. (b) TEM images of MnO/C-1 electrode after 500 cycles.

Fig. S6 Cycle performance and Coulombic efficiency for MnO/C samples at a current density of 5A g^{-1} for 5000 cycles.

Table S2. Comparison with the performance of previously reported Li-ion capacitors

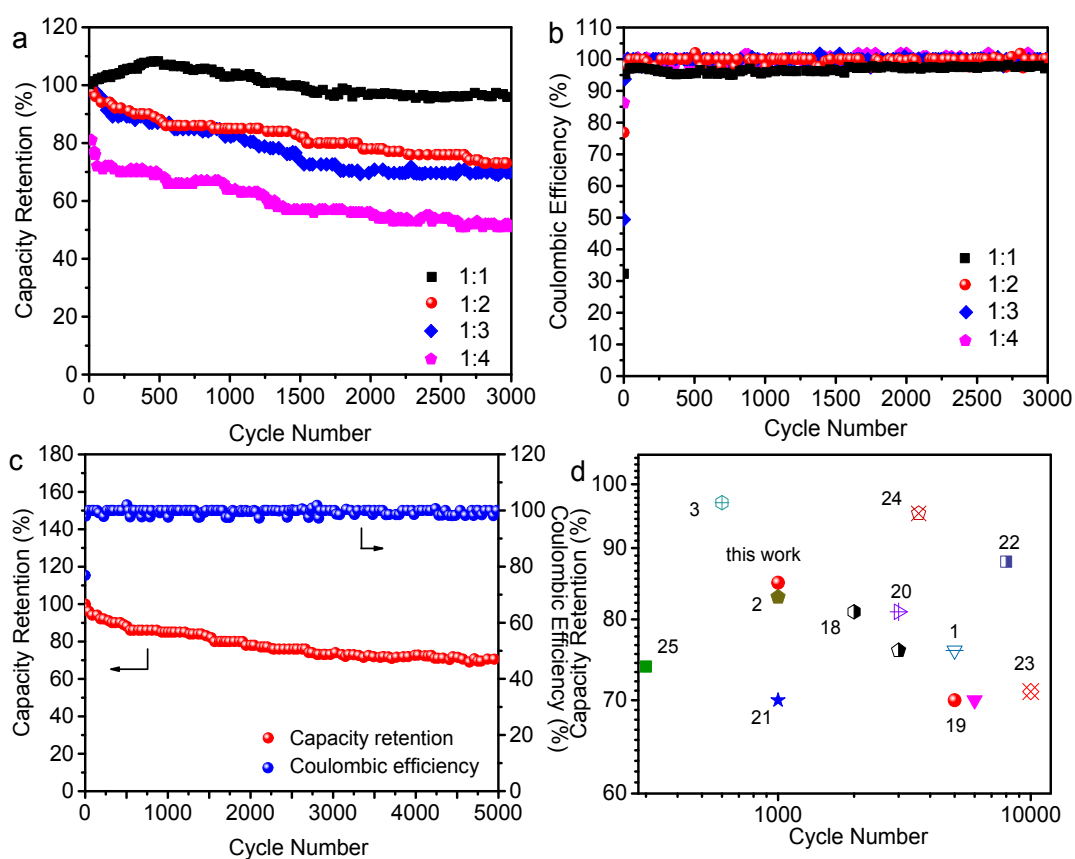| Hybrid System	Votage Window	Electrolyte	Energy Density/Power Density	Reference
MnO/C‖CNS	1.0-4.0 V	1 M LiFP$_6$	100 Wh kg^{-1} at 83 W kg^{-1}; 33650 W kg^{-1} at 21 Wh kg^{-1}	This work
3D-MnO/CNS‖ 3D-CNS	1.0-4.0 V	1M LiPF$_6$	184 Wh kg^{-1} at 83 W kg^{-1}; 18000 W kg^{-1} at 83 Wh kg$^-$	1
3DVN-RGO‖ APDC	0-4.0 V	1 M LiPF$_6$	162 Wh kg^{-1} at 200 W kg^{-1}; 10000 W kg^{-1} at 64 Wh kg$^-$	2
HC‖AC	1.8-3.9 V	1.2 M LiPF$_6$	82 Wh kg^{-1} at 100 W kg^{-1}; 5500 W kg^{-1} at 45 Wh kg^{-1}	3
TiC‖PHPNC	0-4.5 V	1 M LiPF$_6$	101.5 Wh kg^{-1} at 450 W kg^{-1}; 675000 W kg^{-1} at 23.4 Wh kg^{-1}	4
MFC‖ 3DaC	0-4.0 V	1 M LiPF$_6$	157 Wh kg^{-1} at 200 W kg^{-1}; 20000 W kg^{-1} at 58 Wh kg^{-1}	5
LTP‖AC	0-3.0 V	1 M LiPF$_6$	14 Wh kg^{-1} at 45 W kg^{-1}; 180 W kg^{-1} at 0.6 Wh kg^{-1}	6
Li4Ti$_5$O$_{12}$‖ ODC	1.0-3.0 V	1 M LiPF$_6$	60 Wh kg^{-1} at 200 W kg^{-1}; 10000 W kg^{-1} at 9 Wh kg^{-1}	7
LTO‖AC	0.5-3.5 V	1 M LiPF$_6$	90 Wh kg^{-1} at 50 W kg^{-1}; 6000 W kg^{-1} at 32 Wh kg^{-1}	8
C-LTO‖AC	1.5-2.5 V	1 M LiPF$_6$	25 Wh kg^{-1} at 40 W kg^{-1}; 1010 W kg^{-1} at 16 Wh kg^{-1}	9
Li$_4$Ti$_5$O$_{12}$‖ TRGO	1.0-3.0 V	1 M LiPF$_6$	45 Wh kg^{-1} at 400 W kg^{-1}; 3300 W kg^{-1} at 35 Wh kg^{-1}	10
CPIMS900‖ AC	2.0-4.0 V	1 M LiPF$_6$	28.5 Wh kg^{-1} at 348 W kg^{-1}; 6940 W kg^{-1} at 13.1 Wh kg^{-1}	11
MSP20‖ hard carbon	1.4-4.3V	1 M LiFP$_6$	75 Wh kg^{-1} at 750 W kg^{-1}; 2300 W kg^{-1} at 58 Wh kg^{-1}	12
TiO$_2$‖AC	0-2.8 V	1 M LiPF$_6$	79 Wh kg^{-1} at 180 W kg^{-1}; 9450 W kg^{-1} at 32 Wh kg^{-1}	13
Li(Mn$_{1/3}$Ni$_{1/3}$Fe$_{1/3}$)O$_2-$ PANI‖AC	0-3.0 V	1 M LiPF$_6$	49 Wh kg^{-1} at 1 W kg^{-1}; 3 W kg^{-1} at 19 Wh kg^{-1}	14
LMCMB‖ SFAC	2.0-4.0 V	1 M LiPF$_6$	83 Wh kg^{-1} at 128 W kg^{-1}; 5718 W kg^{-1} at 41 Wh kg^{-1}	15
TiO$_2$(reduced graphene oxide‖AC	2.0-4.0 V	1 M LiPF$_6$	42 Wh kg^{-1} at 800 W kg^{-1}; 8000 W kg^{-1} at 8.9 Wh kg^{-1}	16
HC‖AC	2.0-4.0 V	1.2 M LiPF$_6$	85.7 Wh kg^{-1} at 7.6 W kg^{-1}; 8000 W kg^{-1} at 20 Wh kg^{-1}	17

Fig. S7 (a) Cycling performance of MnO/C||CNS Li-ion capacitors with different anode to cathode mass ratios, tested at the current density of 5 A g^{-1}. (b) The correspongding Coulombic efficiency of MnO/C|| CNS Li-ion capacitors. (c) Cycling performance and Coulombic efficiency of MnO/C||CNS Li-ion capacitors with anode to cathode mass ratio of 1:2, tested at the current density of 5 A g^{-1}. (d) Cycling performance comparison of MnO/C||CNS versus reported values for hybrid systems.
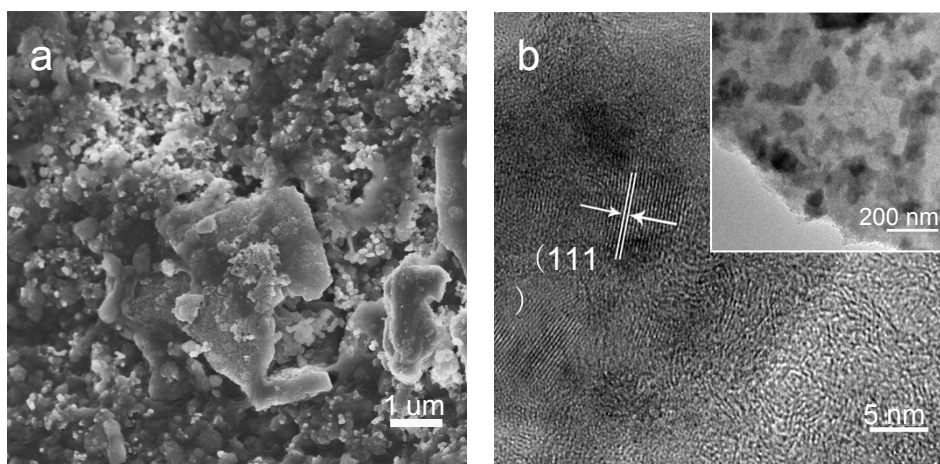
Fig. S8 (a) SEM image and (b) TEM images of the MnO/C electrode for the MnO/C‖CNS Li-ion capacitors with anode to cathode mass ratio of 1:2 after 5000 cycles.
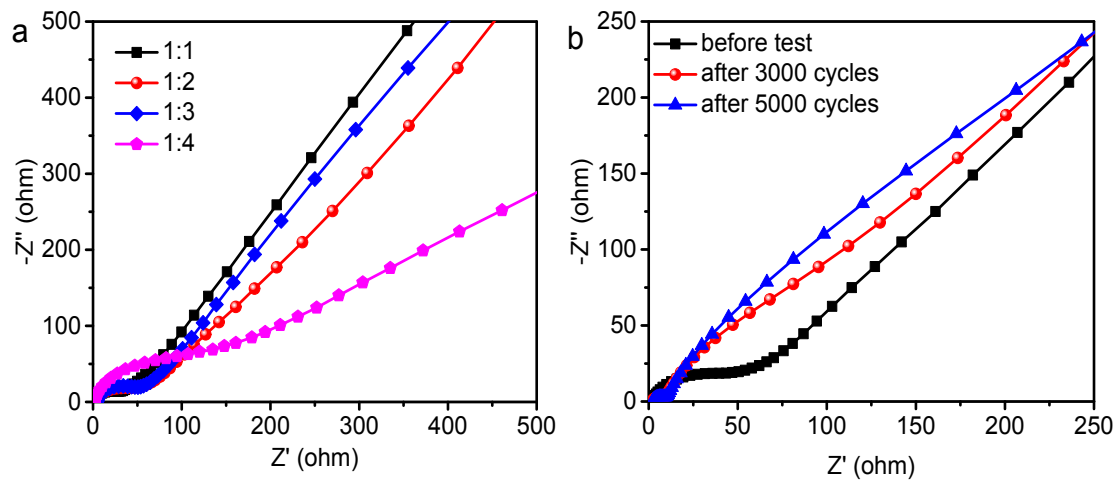
Fig. S9 (a) Electrochemical impedance spectra of Li-ion capacitors before cycling. (b) Electrochemical impedance spectra of Li-ion capacitors with the anode to cathode mass ratio of 1:2 before test, after 3000 cycles and after 5000 cycles.

Notes and references

1 H. Wang, Z. Xu, Z. Li, K. Cui, J. Ding, A. Kohandehghan, X. Tan, B. Zahiri, B. C. Olsen, C. M. Holt and D. Mitlin, *Nano Lett.*, 2014, **14**, 1987-1994.

2 R. Wang, J. Lang, P. Zhang, Z. Lin and X. Yan, *Adv. Funct. Mater.*, 2015, **25**, 2270-2278.

3 W. J. Cao and J. P. Zheng, *J. Power Sources*, 2012, **213**, 180-185.

4 H. Wang, Y. Zhang, H. Ang, Y. Zhang, H. T. Tan, Y. Zhang, Y. Guo, J. B. Franklin, X. L. Wu, M. Srinivasan, H. J. Fan and Q. Yan, *Adv. Funct. Mater.*, 2016, **26**, 3082-3093.

5 W. S. V. Lee, E. Peng, M. Li, X. Huang and J. M. Xue, *Nano Energy*, 2016, **27**, 202-212.

6 V. Aravindan, W. Chuiling, M. V. Reddy, G. V. Rao, B. V. Chowdari and S. Madhavi, *Phys. Chem. Chem. Phys.*, 2012, **14**, 5808-5814.

7 R. Gokhale, V. Aravindan, P. Yadav, S. Jain, D. Phase, S. Madhavi and S. Ogale, *Carbon*, 2014, **80**, 462-471.

8 H. S. Choi, J. H. Im, T. Kim, J. H. Park and C. R. Park, *J. Mater. Chem.* 2012, **22**, 16986-18993.

9 H.-G. Jung, N. Venugopal, B. Scrosati and Y.-K. Sun, *J. Power Sources*, 2013, **221**, 266-271.

10 V. Aravindan, D. Mhamane, W. C. Ling, S. Ogale and S. Madhavi, *ChemSusChem*, 2013, **6**, 2240-2244.

11 X. Han, P. Han, J. Yao, S. Zhang, X. Cao, J. Xiong, J. Zhang and G. Cui, *Electrochim. Acta*, 2016, **196**, 603-610.

12 J.-H. Kim, J.-S. Kim, Y.-G. Lim, J.-G. Lee and Y.-J. Kim, *J. Power Sources*, 2011, **196**, 10490-10495.

13 Y. Cai, B. Zhao, J. Wang and Z. Shao, *J. Power Sources*, 2014, **253**, 80-89.

14 K. Karthikeyan, S. Amaresh, V. Aravindan, H. Kim, K. S. Kang and Y. S. Lee, *J. Mater. Chem. A*, 2013, **1**, 707-714.

15 Z. Yang, H. Guo, X. Li, Z. Wang, Z. Yan and Y. Wang, *J. Power Sources*, 2016,

329, 339-346.

16 H. Kim, M.-Y. Cho, M.-H. Kim, K.-Y. Park, H. Gwon, Y. Lee, K. C. Roh and K. Kang, *Adv. Energy Mater.*, 2013, **3**, 1500-1506.

17 J. Zhang, X. Liu, J. Wang, J. Shi and Z. Shi, *Electrochim. Acta*, 2016, **187**, 134-142.

18 M. Yang, Y. Zhong, J. Ren, X. Zhou, J. Wei and Z. Zhou, *Adv. Energy Mater.*, 2015, **5**, 1500550.

19 R. Yi, S. Chen, J. Song, M. L. Gordin, A. Manivannan and D. Wang, *Adv. Funct. Mater.*, 2014, **24**, 7433-7439.

20 N. Arun, A. Jain, V. Aravindan, S. Jayaraman, W. Chui Ling, M. P. Srinivasan and S. Madhavi, *Nano Energy*, 2015, **12**, 69-75.

21 F. Zhang, T. Zhang, X. Yang, L. Zhang, K. Leng, Y. Huang and Y. Chen, *Energy Environ. Sci.*, 2013, **6**, 1623-1632.

22 B. Li, F. Dai, Q. Xiao, L. Yang, J. Shen, C. Zhang and M. Cai, *Energy Environ. Sci.*, 2016, **9**, 102-106.

23 N. Xu, X. Sun, X. Zhang, K. Wang and Y. Ma, *RSC Adv.*, 2015, **5**, 94361-94368.

24 C. Liu, C. Zhang, H. Song, X. Nan, H. Fu and G. Cao, *J. Mater. Chem. A*, 2016, **4**, 3362-3370.

25 J. J. Ren, L. W. Su, X. Qin, M. Yang, J. P. Wei, Z. Zhou and P. W. Shen, *J. Power Sources*, 2014, **264**, 108-113.